

FINAL REPORT
ESEERCO PROJECT EP 95-11

Real Time Control of Oscillations of Electric Power Systems

September 1996

Prepared by:

Power Systems Engineering Research Consortium (PSerc)
Cornell University
Ithaca, NY 14853

Principal Investigators:

Pete Sauer, M. A. Pai, Stephen Fernandes
Ian Dobson, Fernando Alvarado, Scott Greene
Bob Thomas, Hsiao-Dong Chiang

Prepared for:

Empire State Electric Energy Research Corporation
1515 Broadway, 43rd Floor
New York, New York 10036-5701

and

New York State Electric & Gas

Copyright @ 1996
EMPIRE STATE ELECTRICAL ENERGY RESEARCH CORPORATION
AND CORNELL UNIVERSITY.
All Rights reserved

LEGAL NOTICE

This report was prepared as an account of work sponsored by the Empire State Electric Energy Research Corporation ("ESEERCO") and New York State Electric and Gas Corporation ("NYSEG"). Neither ESEERCO, members of ESEERCO, NYSEG nor any person acting on behalf of any of them:

- a. Makes any warranty or representation, express or implied, with respect to the accuracy, completeness, or usefulness of the information contained in this report, or that the use of any information, apparatus, method, or process disclosed in this report may not infringe on privately owned rights; or
- b. Assumes any liability with respect to the use of, or for damages resulting from the use of, any information, apparatus, method, or process disclosed in this report.

Prepared by Cornell University, Ithaca, New York

Acknowledgements

The authors gratefully acknowledge the interest and support of the Empire State Electric Energy Research Corp. and New York State Electric and Gas.

Contents

1	Introduction	1
2	The Dynamic Model for Test Cases	2
3	Sensitivity of critical mode eigenvalues	4
4	Closeness to the Onset of Oscillation and its Sensitivity	7
4.1	Measuring the closeness to onset of oscillations with a margin M	7
4.2	Computing the margin M with a continuation method	8
4.3	The sensitivity of M to parameters	9
5	Single Machine Results	10
5.1	Test case system and data	10
5.2	Validation of margin sensitivity	12
5.3	Validation of the control effectiveness	13
6	37 Bus Equivalent Results	16
6.1	37 bus equivalent test case system and data	16
6.2	Eigenvalue analysis for load increase	16
6.3	Eigenvalue analysis - line outage	17
7	Computational Issues	18
8	Conclusions	18
A	Appendix A	21
B	Appendix B	22

List of Figures

1	Normal vector and margin to the surface of critical parameter values	8
2	Schematic of the single machine infinite bus system test case	11
3	Margin to Oscillatory Instability vs. Parameter	13

List of Tables

1	Machine and System Data	12
2	Excitation System Data	12
3	Governor-Steam Turbine Data	12
4	Eigenvalues and sensitivities with respect to P_C at Hopf bifurcation	14
5	Eigenvalues when P_C is changed by -0.0065 predicted	14
6	Eigenvalues and sensitivities with respect to V_{ref} at Hopf bifurcation	15
7	Eigenvalues when V_{ref} is changed by 0.0023 predicted	15
8	Critical eigenvalues and their sensitivities	16

Executive Summary

Contingencies or extreme system loading can cause unacceptable power system operating conditions such as low voltages, excessive line flows, or dynamic instabilities. The real-time controls needed to eliminate low voltages or excessive line flows are reasonably well understood either based on experience or apriori operator guidelines. In contrast, real-time control strategies for dynamic instabilities are much less mature. Unbounded dynamic instabilities can cause rapid damage to equipment, usually providing insufficient time for operator control. Automatic protective devices are assumed to provide the necessary real-time control. When dynamic instabilities are bounded, they appear as sustained oscillations or limit cycles which may not cause protective devices to operate and therefore may require operator intervention to suppress them. A number of utilities have experienced these problems and heuristic methods to eliminate the oscillations have had limited success.

This project investigated the feasibility of an approach to provide operator assistance in the prediction and suppression of sustained system oscillations. The primary thrust of the project was based on a real-time simulation which would track the system dynamic behavior. The monitor for the closeness of the system to the onset of oscillations would be based on an indicator which provides a measure of the distance to oscillatory instability in terms of total load. The methods for suppressing sustained system oscillations were to be based on eigenvalue sensitivity techniques which can provide a ranking of various control options.

Results on a single machine/infinite bus system show that the concept is viable. Results on a 37 bus equivalent system do not indicate feasibility for large-scale systems. The results indicate that eigenvalue movement in response to typical operation controls can be sufficiently nonlinear to make prediction of remedial action unreliable. These and other computational issues are discussed in the following sections.

1 Introduction

Sustained oscillations normally arise when a dynamic system evolves such that its equilibrium point is unstable - normally due to a complex pair of eigenvalues in the right-half plane. The onset of this oscillatory instability occurs when the pair of eigenvalues lies on the imaginary axis of the complex plane. This onset of instability is also called a Hopf bifurcation and the main objective of the project was to avoid or suppress these oscillations with real time controls.

This project assumed that a simulation is tracking the behavior of the actual system in real-time. The simulation would obtain real-time data from the system state estimator and compute the system equilibrium point in terms of the dynamic model states. (This is a straightforward calculation provided a full load flow state estimate is provided together with real-time dynamic model parameter information.) The project examined the development of computations for selecting real time controls to avoid or suppress system oscillations. The main approach was to select controls by determining the sensitivity of the measures of closeness to the onset of oscillations. Two measures of closeness are the damping of the critical eigenvalues (oscillatory mode) and the loading margin (increment in loading) to the onset of oscillations.

This report presents a method for computing eigenvalue sensitivities with respect to different system parameters. For many parameters of interest for real time control, the Jacobian depends on the parameter implicitly via the dependence of the operating equilibrium on the parameters. One novel feature of this project is that full account is taken of this implicit dependence in computing sensitivities. The report also explains measuring the closeness to the Hopf bifurcation with a margin related to system loading. For example, the margin can be the additional system load required for the oscillations to begin. The sensitivity of the margin to parameters can be computed. The sensitivities of critical eigenvalue damping or the margin can be used to select controls which avoid or suppress the oscillations. At this stage, these controls are limited to basic continuous controls such as voltage and speed set points. The sensitivities can also be used to find out how accurately all the system parameters need to be known to adequately predict the oscillations.

The parameters chosen are the generator set points, typically, the power change setting P_C of a mechanical-hydraulic governor speed controller and the reference voltage set point V_{ref} . Unlike most other methods the proposed approach is easily applicable to detailed generator models (no model order reductions are necessary) and to different computational schemes for calculating the eigenvalue sensitivity ([14],[10],[6],[19]). Examples of a single machine infinite bus test system are presented as an initial illustration of the proposed scheme. The margin to the Hopf bifurcation is measured and its sensitivity to parameter change is computed. Sensitivities of critical eigenvalues at and around the Hopf bifurcation point are computed and the results are used to damp out sustained oscillations in the test system.

Computational schemes for computing eigenvalues and eigenvectors for large power systems have been presented in [22],[20],[21],[2],[10],[12]. Most literature dealing with sensitivity analysis applied to power systems ([14],[19]) assumes that the parameter only appears explicitly in the system Jacobian. This assumption is not made here. One important paper analyzing oscillations in small power system examples as Hopf bifurcations is [1].

There are two types of Hopf bifurcation: supercritical and subcritical. When the oscillatory instability arises due to a super-critical Hopf bifurcation, the response appears naturally as bounded oscillations (not due to the enforcement of hard limits). When the instability arises due to a subcritical Hopf bifurcation, the response appears as growing oscillations. If the system model has hard limits on system devices or controls,

then these growing oscillations can be bounded as the limits prevent growth. Since this project is concerned with the prediction and elimination of sustained oscillations, we are not seriously concerned about which of these two mechanism produces a given sustained oscillation.

2 The Dynamic Model for Test Cases

The dynamic model for the test cases in this project consists of fourth-order synchronous machines (angle, speed, field flux, one damper winding) with IEEE type I excitation systems (third order), and first-order models each for turbines, boilers, and governors. The model for each machine i is:

$$\frac{d\delta_i}{dt} = \omega_i - \omega_s \quad (1)$$

$$\frac{d\omega_i}{dt} = \frac{T_{Mi}}{M_i} - \frac{[E'_{qi} - X'_{di}I_{di}]I_{qi}}{M_i} - \frac{[E'_{di} + X'_{qi}I_{qi}]I_{di}}{M_i} - \frac{D_i(\omega_i - \omega_s)}{M_i} \quad (2)$$

$$\frac{dE'_{qi}}{dt} = -\frac{E'_{qi}}{T'_{doi}} - \frac{(X_{di} - X'_{di})I_{di}}{T'_{doi}} + \frac{E_{fdi}}{T'_{doi}} \quad (3)$$

$$\frac{dE'_{di}}{dt} = -\frac{E'_{di}}{T'_{qoi}} + \frac{I_{qi}(X_{qi} - X'_{qi})}{T'_{qoi}} \quad (4)$$

$$\frac{dE_{fdi}}{dt} = -\frac{K_{Ei} + S_{Ei}(E_{fdi})}{T_{Ei}}E_{fdi} + \frac{V_{Ri}}{T_{Ei}} \quad (5)$$

$$\frac{dV_{Ri}}{dt} = -\frac{V_{Ri}}{T_{Ai}} + \frac{K_{Ai}}{T_{Ai}}R_{Fi} - \frac{K_{Ai}K_{Fi}}{T_{Ai}T_{Fi}}E_{fdi} + \frac{K_{Ai}}{T_{Ai}}(V_{refi} - V_i) \quad (6)$$

$$\frac{dR_{Fi}}{dt} = -\frac{R_{Fi}}{T_{Fi}} + \frac{K_{Fi}}{T_{Fi}^2}E_{fdi} \quad (7)$$

$$\frac{dT_{Mi}}{dt} = -\frac{T_{Mi}}{T_{RH_i}} + \left(\frac{1}{T_{RH_i}} - \frac{K_{HP_i}}{T_{CH_i}} \right) P_{CH_i} + \frac{K_{HP_i}}{T_{CH_i}} P_{SV_i} \quad (8)$$

$$\frac{dP_{CH_i}}{dt} = -\frac{P_{CH_i}}{T_{CH_i}} + \frac{P_{SV_i}}{T_{CH_i}} \quad (9)$$

$$\frac{dP_{SV_i}}{dt} = -\frac{P_{SV_i}}{T_{SV_i}} + \frac{P_{Ci}}{T_{SV_i}} - \frac{1}{R_{di}T_{SV_i}} \left(\frac{\omega_i}{\omega_s} - 1 \right) \quad (10)$$

where

$$S_{Ei}(E_{fdi}) = A_{exi} e^{B_{exi} E_{fdi}}, \quad M_i = \frac{2H_i}{\omega_s} \quad (11)$$

$$\omega_s = 2\pi \cdot 60 \quad (12)$$

and the following limit constraints apply:

$$V_{Ri}^{min} \leq V_{Ri} \leq V_{Ri}^{max} \quad \text{and} \quad 0 \leq P_{SV_i} \leq P_{SV_i}^{max} \quad i = 1, \dots, m \quad (13)$$

Stator Algebraic Equations

The stator algebraic equations in polar form are

$$E'_{di} - V_i \sin(\delta_i - \theta_i) - R_{si} I_{di} + X'_{qi} I_{qi} = 0 \quad (14)$$

$$E'_{qi} - V_i \cos(\delta_i - \theta_i) - R_{si} I_{qi} - X'_{di} I_{di} = 0 \quad i = 1, \dots, m \quad (15)$$

Network Equations

The network equations are

$$I_{di} V_i \sin(\delta_i - \theta_i) + I_{qi} V_i \cos(\delta_i - \theta_i) + P_{Li}(V_i) - \sum_{k=1}^n V_i V_k Y_{ik} \cos(\theta_i - \theta_k - \alpha_{ik}) = 0 \quad (16)$$

$$I_{di} V_i \cos(\delta_i - \theta_i) - I_{qi} V_i \sin(\delta_i - \theta_i) + Q_{Li}(V_i) - \sum_{k=1}^n V_i V_k Y_{ik} \sin(\theta_i - \theta_k - \alpha_{ik}) = 0 \quad (17)$$

$i = 1, \dots, m$

$$P_{Li}(V_i) - \sum_{k=1}^n V_i V_k Y_{ik} \cos(\theta_i - \theta_k - \alpha_{ik}) = 0 \quad (18)$$

$$Q_{Li}(V_i) - \sum_{k=1}^n V_i V_k Y_{ik} \sin(\theta_i - \theta_k - \alpha_{ik}) = 0 \quad i = m + 1, \dots, n \quad (19)$$

where $P_{Li}(V_i)$ and $Q_{Li}(V_i)$ represent the load models.

The differential-algebraic model above can be summarized as

$$\dot{x} = f(x, y, p) \quad (20)$$

$$0 = g(x, y, p) \quad (21)$$

where x is the vector containing the n_x differential states and y is the vector containing the n_y algebraic states, p is the vector containing all parameters:

$$x = (\delta, \omega, E'_q, E'_d, E_{fd}, V_R, R_F, T_M, P_{CH}, P_{SV})^t \quad (22)$$

$$y = (V, \theta, I_d, I_q)^t \quad (23)$$

$$p = (P_C, V_{ref})^t \quad (24)$$

where δ stands for $\delta_1, \delta_2, \dots, \delta_m$ and ω stands for $\omega_1, \omega_2, \dots, \omega_m$ and similarly for the remaining states and parameters.

It is convenient to rewrite (20),(21) as

$$\begin{pmatrix} \dot{x} \\ 0 \end{pmatrix} = \begin{pmatrix} f(x, y, p) \\ g(x, y, p) \end{pmatrix} \quad (25)$$

or

$$I_o \dot{z} = G(z, p) \quad (26)$$

where

$$z = \begin{pmatrix} x \\ y \end{pmatrix} \quad (27)$$

$$I_o = \begin{pmatrix} I_{n_x \times n_x} & O_{n_x \times n_y} \\ O_{n_y \times n_x} & O_{n_y \times n_y} \end{pmatrix} \quad (28)$$

$$G(z, p) = \begin{pmatrix} f(x, y, p) \\ g(x, y, p) \end{pmatrix} \quad (29)$$

3 Sensitivity of critical mode eigenvalues

The background and formulas for the eigenvalue sensitivity are now presented. Discussion of technical mathematical assumptions is postponed to the end of the section. The derivation combines together approaches from ([6],[15],[10],[19])

Differential equations can be obtained from the differential algebraic model (20) and (21) by eliminating the algebraic states y . Solving the algebraic equations (21) for y in terms of x yields a function

$$y = h(x, p) \quad (30)$$

Substitution of $h(x, p)$ for y in (20) yields the differential equations

$$\dot{x} = f(x, h(x, p), p) \quad (31)$$

$$= F(x, p) \quad (32)$$

Superscripts are used to indicate the i th component of a vector. For example the i th component of the vector x is x^i and the i th equation of (32) is

$$\dot{x}^i = F^i(x, p) \quad (33)$$

Since h was derived by solving the algebraic equations (21),

$$0 = g(x, h(x, p), p) \quad (34)$$

The Jacobian h_x of h with respect to x is obtained by differentiating (34):

$$0 = g_x + g_y h_x \quad (35)$$

$$h_x = -g_y^{-1} g_x \quad (36)$$

Now the system Jacobian F_x can be expressed in terms of f and g by differentiating (32):

$$F_x = f_x + f_y h_x = f_x - f_y g_y^{-1} g_x \quad (37)$$

The system eigenvalues are the eigenvalues of the Jacobian matrix F_x . Let λ be one of these eigenvalues and let v and w be the right and left eigenvectors associated with λ . w is a row vector and v is a column vector.

Write

$$\bar{v} = \begin{pmatrix} v \\ h_x v \end{pmatrix} = \begin{pmatrix} v \\ -g_y^{-1} g_x v \end{pmatrix} \quad (38)$$

Then, using (37)

$$G_z \bar{v} = \begin{pmatrix} f_x & f_y \\ g_x & g_y \end{pmatrix} \begin{pmatrix} v \\ -g_y^{-1} g_x v \end{pmatrix} = \begin{pmatrix} (f_x - f_y g_y^{-1} g_x) v \\ 0 \end{pmatrix} = \begin{pmatrix} F_x v \\ 0 \end{pmatrix} = \lambda \begin{pmatrix} v \\ 0 \end{pmatrix} = \lambda I_o \bar{v} \quad (39)$$

Similarly, write

$$\bar{w} = (w, -w f_y g_y^{-1}) \quad (40)$$

and obtain

$$\bar{w} G_z = (w, -w f_y g_y^{-1}) \begin{pmatrix} f_x & f_y \\ g_x & g_y \end{pmatrix} = (w(f_x - f_y g_y^{-1} g_x), 0) = (w F_x, 0) = \lambda (w, 0) = \lambda \bar{w} I_o \quad (41)$$

The vector \bar{v} defines the mode shape of both the differential and algebraic variables in the same way as the eigenvector v defines the mode shape of the differential variables. (The equation $G_z \bar{v} = \lambda I_o \bar{v}$ is called a generalized eigenvalue problem [8], [19].)

The operating point or equilibrium of (26) is written as $Z(p)$ and satisfies

$$0 = G(Z(p), p) \quad (42)$$

The equilibrium $Z(p)$ is a function of the parameter p . The sensitivity of this equilibrium with respect to p is the vector $Z_p = \frac{\partial Z}{\partial p}$ which can be evaluated by differentiating (42) and rearranging terms:

$$0 = G_z Z_p + G_p \quad (43)$$

$$Z_p = -(G_z)^{-1} G_p \quad (44)$$

The i th components of equations (43) and (44) can be written as

$$0 = \sum_j \frac{\partial G^i}{\partial z^j} Z_p^j + \frac{\partial G^i}{\partial p} \quad (45)$$

$$Z_p^i = - \sum_j [(G_z)^{-1}]^{ij} \frac{\partial G^j}{\partial p} \quad (46)$$

For practical computation of Z_p , explicit evaluation of the inverse $(G_z)^{-1}$ is avoided and sparse methods are used.

In the differential-algebraic equations (26), G is a function of z and p . Therefore the Jacobian of the differential-algebraic equations $G_z(z, p)$ is also a function of z and p . When the Jacobian of the differential-algebraic equations is evaluated at the equilibrium $Z(p)$, it can be regarded as function $J(p)$ of p :

$$J(p) = G_z(Z(p), p) \quad (47)$$

That is, J varies with the parameter p , not only because the entries of the Jacobian might depend directly on p but also because the equilibrium position $Z(p)$ might vary with p and the Jacobian is evaluated at $Z(p)$.

Evaluating (39) and (41) at $(Z(p), p)$ gives

$$J \bar{v} = \lambda I_o \bar{v} \quad (48)$$

$$\bar{w} J = \lambda \bar{w} I_o \quad (49)$$

and hence

$$0 = \bar{w}(J - \lambda I_o)\bar{v} \quad (50)$$

To obtain the eigenvalue sensitivity, differentiate (50) with respect to p to obtain

$$0 = \bar{w}(J_p - \lambda_p I_o)\bar{v} \quad (51)$$

(The other terms involving \bar{v}_p and \bar{w}_p vanish). Rearrangement of (51) and using $\bar{w}I_o\bar{v} = wv$ gives a formula for the eigenvalue sensitivity $\lambda_p = \frac{\partial \lambda}{\partial p}$ with respect to the parameter p :

$$\lambda_p = \frac{\bar{w}J_p\bar{v}}{wv} = \frac{\sum_{i,j} \bar{w}^i J_p^{ij} \bar{v}^j}{\sum_i w^i v^i} \quad (52)$$

It remains to express J_p^{ij} in terms of derivatives of G . The i, j component of equation (47) is

$$J^{ij}(p) = G_z^{ij}(Z(p), p) = \frac{\partial G^i}{\partial z^j}(Z(p), p) \quad (53)$$

Differentiate (53) with respect to p to obtain

$$J_p^{ij} = \sum_k \frac{\partial^2 G^i}{\partial z^j \partial z^k} Z_p^k + \frac{\partial^2 G^i}{\partial z^j \partial p} \quad (54)$$

and substitute in (52) to finally obtain the eigenvalue sensitivity formula

$$\lambda_p = \frac{\sum_{i,j,k} \bar{w}^i \frac{\partial^2 G^i}{\partial z^j \partial z^k} Z_p^k \bar{v}^j + \sum_{i,j} \bar{w}^i \frac{\partial^2 G^i}{\partial z^j \partial p} \bar{v}^j}{\sum_i w^i v^i} \quad (55)$$

The first term in (55) describes first order changes in the eigenvalue λ due to changes in p affecting the equilibrium position at which the Jacobian is evaluated and the second term describes first order changes in λ due to changes in p affecting the entries of the Jacobian directly.

There are some technical assumptions required to make the procedure above rigorous:

- The limits (13) are neglected to ensure that f and g are smooth functions.
- The construction of the function h in (30) requires g_y to be assumed invertible. According to the implicit function theorem, h is well defined locally if g_y is invertible. The construction of \bar{w} and \bar{v} also requires g_y to be invertible.
- The eigenvalue λ is assumed to be unique and simple. The simplicity of λ ensures that $wv \neq 0$ so that the division by wv in (55) is valid. The uniqueness of λ ensures that w and v are unique up to scaling by a constant.
- The computation of Z_p requires that G_z is invertible (see (44)).

4 Closeness to the Onset of Oscillation and its Sensitivity

This section explains how to compute the closeness or margin to onset of oscillation and the sensitivity of this margin to parameters.

4.1 Measuring the closeness to onset of oscillations with a margin M

The closeness to the onset of oscillation is measured by the change in one of the parameters required for the system to be at the onset of oscillation. Suppose the change in parameter is M (M stands for *M*argin to onset of oscillation). The choice of which parameter is used for M must be made according to which parameter is most meaningful as a measure of closeness. For example, in the single machine infinite bus example, the parameter P_C describes (in some sense) the system loading and the change in P_C could be a good choice for M . In this case, $M = P_C$ would describe the increase in loading before the onset of oscillations. In a multibus system with several areas, it might be appropriate to choose M as the change in a critical interarea flow. In this case, M would describe an increase in this interarea flow which would lead to the onset of oscillations. Alternatively, system loading in a multibus system could be used as a margin by picking a specific pattern of load increase and then defining M to be the amount of load increase in that specific pattern.

To explain and define the margin M more precisely, suppose that the power system has an equilibrium when the parameters are p_0 . Suppose first that M is chosen to reflect changes in the first parameter in the vector p . Define the unit vector

$$k = \begin{pmatrix} 1 \\ 0 \\ \vdots \\ 0 \end{pmatrix} \quad (56)$$

(a more general choice of k is used below) and consider p changing from p_0 according to

$$p = p_0 + mk \quad (57)$$

as the scalar m increases from zero. Suppose that as m increases, the first onset of instability occurs at p_* . Then M is defined so that

$$p_* = p_0 + Mk \quad (58)$$

That is,

$$M = k^T (p_* - p_0) \quad (59)$$

Thus when k is given by (56), M measures the change of the first parameter from its value at p_0 to its value at the onset of oscillations at p_* .

It is now straightforward to allow a more general choice of the unit vector k to allow for the individual or joint variation of other parameters when defining M . If (56) is replaced by a more general choice of k , then equations (57,58,59) immediately apply and now M measures the change of the parameter p in the direction k from its value at p_0 to its value at the onset of oscillations at p_* . This is illustrated in the case of the vector p containing two parameters in Figure 1

In the case of a power system with many loads which are represented by their real and reactive power demands appearing as parameters in the model, k could be thought of as defining the pattern or direction

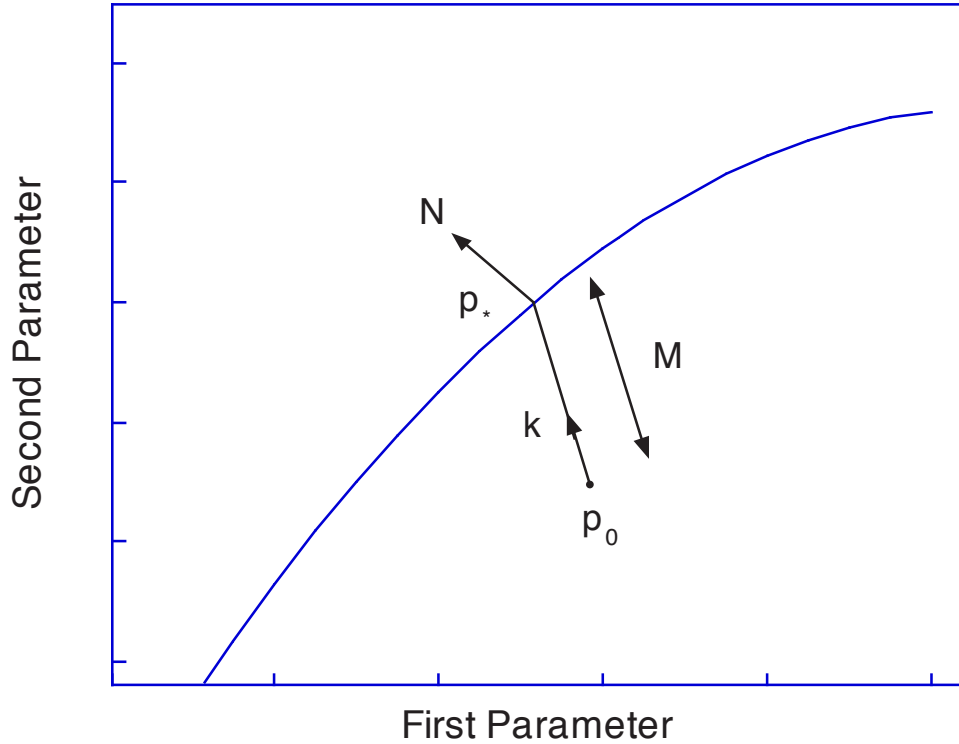


Figure 1: Normal vector and margin to the surface of critical parameter values

of load increase. In this case M measures the margin to the onset of oscillations as loads increase in the proportions indicated by the entries of k .

The margin M can be useful either when the system is stable or unstable when the parameters are p_0 . If p_0 corresponds to a stable operating equilibrium, then M is the margin to p_0 becoming oscillatory unstable at p_* . In this case one would usually set up the definition of M so that the M is positive. If p_0 is oscillatory unstable, then the power system cannot operate at p_0 . (However, it is quite likely that the power system is oscillating around p_0 .) However, the closeness of the parameters p_0 to parameters p_* at which the oscillatory instability of the equilibrium is first suppressed can be measured with a margin M . It is possible to set up the definition of M so that M would be negative in this case. Thus the margin M can be used to measure the “distance to the onset of oscillations in parameter space” when the equilibrium is either stable or unstable.

4.2 Computing the margin M with a continuation method

The main idea of a continuation method is to repeatedly calculate equilibrium solutions as the parameter varies in small steps. The parameter variation is determined by the direction of parameter variation k and the step size Δm . The parameter variation continues until the onset of oscillations is reached. The value of the parameter at the onset of oscillations then determines the margin M .

That is, the continuation begins by computing the equilibrium $Z(p_0)$ and then computes $Z(p_0 + \Delta mk)$,

$Z(p_0 + 2\Delta mk)$, $Z(p_0 + 3\Delta mk)$, \dots . Each equilibrium is checked for oscillatory instability and the continuation ends when the onset of oscillations has been reached. For example, if $Z(p_0 + (i - 1)\Delta mk)$ is a stable equilibrium and $Z(p_0 + i\Delta mk)$ is oscillatory unstable, then the onset of oscillations occurs between $p_0 + (i - 1)\Delta mk$ and $p_0 + i\Delta mk$ and the margin M must satisfy $(i - 1)\Delta m \leq M \leq i\Delta m$. The estimate of M can then be refined by locating the onset of oscillations more exactly.

There are three numerical tasks to be addressed when computing M using continuation:

1. Efficiently compute the successive equilibria as the parameter is incremented.
2. Detect the onset of oscillations between steps
3. Locate the onset of oscillations to the desired accuracy

There is an extensive body of numerical analysis which addresses these tasks; a good general reference is [18].

4.3 The sensitivity of M to parameters

Suppose that the power system is operating at a stable equilibrium corresponding to the vector of parameters p_0 and that the margin M to the onset of oscillations at p_* has been determined. The objective is to change some of the parameters in p_0 to increase M in order to improve the system security. Then it is useful to compute the sensitivity M_{p_0} of the margin M to variation of the parameters p_0 [6]. M_{p_0} is a vector whose i th component is the sensitivity of M with respect to the i th parameter in the vector p_0 . M_{p_0} quantifies to first order the effect on M of changing each parameter in p_0 and knowledge of M_{p_0} allows the most effective parameters to be selected. (M_{p_0} is also useful if the power system has an unstable equilibrium corresponding to p_0 and the objective is to choose parameter changes to stabilize the unstable equilibrium.)

The sensitivity M_{p_0} can be easily computed from eigenvalue sensitivities λ_p evaluated at p_* . (Formulas for λ_p are given in (55)). Define the vector

$$N = \text{Re}\{\lambda_p(p_*)\} \quad (60)$$

(Re means real part.) Then it can be shown [6, 5] that M_{p_0} is simply a scaled version of N :

$$M_{p_0} = \frac{-N}{Nk} = \frac{-N}{\sum_j N^j k^j} \quad (61)$$

Thus the margin sensitivity M_{p_0} is very easy to compute from eigenvalue sensitivities at the onset of oscillations p_* .

Formula (61) can be clarified by explaining the geometric meaning of the vector N . First suppose that there are only two parameters. Figure 1 shows a conceptual sketch of the parameter plane which is divided in two by a curve of critical parameters corresponding to the onset of oscillations. This curve is also called the Hopf bifurcation set. Parameters which yield a stable operating equilibrium such as p_0 are those on one side of the curve and parameters which yield an oscillatory unstable equilibrium are those on the other side of the curve.

Since parameter values on the curve correspond to the onset of oscillations, the real part of a particular system eigenvalue λ must vanish. Indeed, this property defines an equation for the curve:

$$0 = \text{Re}\{\lambda(p)\} \quad (62)$$

The normal vector to the curve is obtained by differentiating (62) with respect to p :

$$\text{normal vector at } p_* = \frac{d}{dp}\text{Re}\{\lambda(p)\}(p_*) = \text{Re}\{\lambda_p(p_*)\} = N \quad (63)$$

Thus N is a vector normal to the critical curve of parameters. Equation (63) relates the eigenvalue sensitivity $\lambda_p(p_*)$ to the geometry of the curve. A normal vector to the curve defines an efficient direction to change parameters to move away from the curve and this fact underlies the appearance of N in (61).

In practical power systems there are many parameters so that the parameter space is multidimensional. Now the critical set of parameters which correspond to the onset of oscillations is a hypersurface (a surface of dimension one less than the number of parameters; for example, if there are two parameters, the hypersurface is the one dimensional curve of Figure 1; if there are three parameters, the hypersurface is a two dimensional surface; if there are 100 parameters, the hypersurface is a 99 dimensional surface). The equations above and the interpretation of N as a normal vector to the hypersurface remain valid. Indeed, it is in the multidimensional case of many parameters that the computations are most useful in assisting the engineering choice of which parameters are best to increase the margin.

5 Single Machine Results

This section presents results for a single machine/infinite bus test system. The results show that the concept is viable for this case.

5.1 Test case system and data

The test case system used in Task 1 is a single machine infinite bus system as shown in Figure 2 with the data of Tables 1-3.

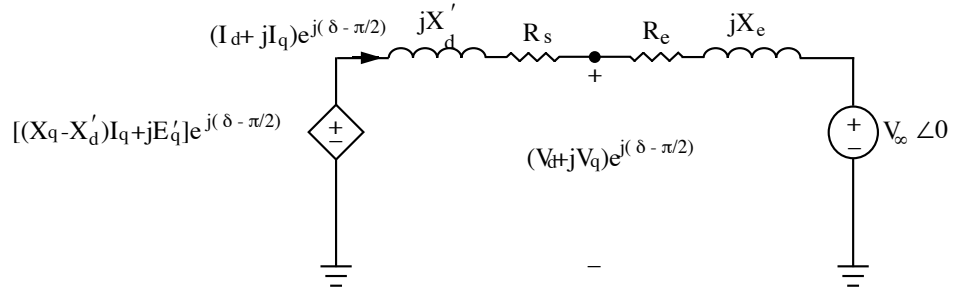


Figure 2: Schematic of the single machine infinite bus system test case

For the test case, the network equations can be simplified to:

$$R_e I_d - X_e I_q - V \sin(\delta - \theta) + V_\infty \sin \delta = 0 \quad (64)$$

$$X_e I_d + R_e I_q - V \cos(\delta - \theta) + V_\infty \cos \delta = 0 \quad (65)$$

The Single Machine Infinite Bus Test Case Data

Table 1: Machine and System Data

R_s	X_d	X_q	X'_d	X'_q
0.00185 p.u.	1.942 p.u.	1.921 p.u.	0.330 p.u.	0.507 p.u.
T'_{do}	T'_{qo}	H	D	$Re + jXe$
5.330 sec	0.593 sec	2.8323 sec	0.0 p.u.	0.001+j0.5 p.u.

Table 2: Excitation System Data

K_A	T_A	K_E	T_E	K_F
50 p.u.	0.02 sec.	1.0 p.u.	0.78 sec.	0.01 p.u.
T_F	A_{ex}	B_{ex}	V_{max}	V_{rmin}
1.2 sec.	0.397 p.u.	0.09 p.u.	9.9 p.u.	-8.9 p.u.

Table 3: Governor-Steam Turbine Data

T_{RH}	K_{HP}	T_{CH}	T_{SV}	R_d
10.0 sec.	0.26 p.u.	0.5 sec.	0.2 sec.	0.05 p.u.

5.2 Validation of margin sensitivity

The single machine example has only two parameters P_C and V_{ref} . (These parameters are measured in per unit.) The power system has a stable equilibrium when $P_C = 1.0$ and $V_{ref} = 0.9547$ and these values are plotted as a point labelled “nominal” in Figure 3.

P_C is varied from 1.0 until the onset of oscillations occurs at $P_{C*} = 1.1497$ (V_{ref} is held constant at 0.9547). The margin M to the onset of oscillations is measured with the change in P_C :

$$M = P_{C*} - 1.0 \quad (66)$$

(In the more general notation of section 4.1, $p_0 = (1.0, 0.9547)^t$, $p_* = (P_{C*}, 0.9547)^t$, $k = (1, 0)^t$.) For the nominal values of $P_C = 1.0$ and $V_{ref} = 0.9547$, (P_{C*} is computed to be 1.1497 and hence the margin is $M = 0.1497$).

The sensitivity in the margin M with respect to V_{ref} was computed using formulas (33). This sensitivity was used to plot the straight line through the nominal point in Figure 3. Thus the margin sensitivity formulas give a linear approximation to the changes in M resulting from changes in V_{ref} at the stable equilibrium. The computed margin sensitivity was validated by computing the exact margin for several values of V_{ref} ; these are plotted as large dots in Figure 3.

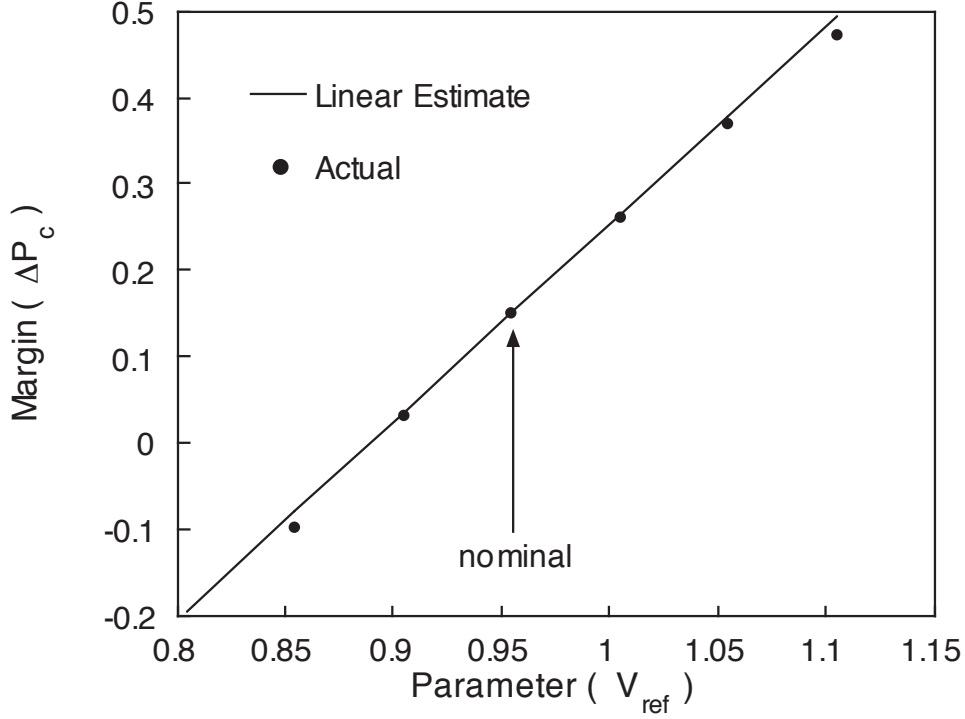


Figure 3: Margin to Oscillatory Instability vs. Parameter

5.3 Validation of the control effectiveness

The single machine infinite bus test system described in section 5.1 was used to validate the eigenvalue sensitivity formulas. A Hopf bifurcation (onset of oscillations) was located when the parameters were $P_C=1.1497$ p.u. and $V_{ref}=0.9547$ p.u. and the system eigenvalues were computed as shown in Table 4. Note the zero real part of the second eigenvalue which confirms that the system is at a Hopf bifurcation. In this section, all eigenvalues have units s^{-1} , all angles have units of radians and all other quantities are per unit. The eigenvalue sensitivities were computed using the formulas of section 3 and are shown in Table 4. These sensitivities were used to predict the eigenvalues when P_C was changed by -0.0065 by linear extrapolation:

$$\lambda(\text{predicted}) = \lambda(\text{Hopf}) - 0.0065 \frac{\partial \lambda}{\partial P_C}(\text{Hopf}) \quad (67)$$

and the results are shown in Table 5 and compared with the actual eigenvalues when P_C was changed by -0.0065 .

Similar results obtained by varying V_{ref} instead of P_C are shown in Tables 6 and 7.

The critical eigenvalues and their sensitivities with respect to P_C and V_{ref} were computed at three equilibria A,B,C as shown in Table 8. The critical eigenvalues show that equilibrium A is stable, equilibrium B is marginally stable and is at a Hopf bifurcation, and that equilibrium C is unstable. (In this context, the critical eigenvalues are defined to be those with the largest (most positive) real part.)

The nonlinear system is now simulated from the unstable equilibrium point C (using a perturbation in one of the differential states). The system breaks into sustained bounded oscillations after about 20 seconds. The oscillations are allowed to continue till at $t = 21^+$ seconds corrective action (as suggested by sensitivity analysis) is applied. The simulation results confirming the effectiveness of the corrective action based on the sensitivities are shown in 3 figures which are not included in this electronic version because of the large size of the data files. The 3 figures may be obtained from the authors. (The 3 figures show the oscillation being successfully damped with corrective actions of changing both P_C and V_{ref} to be equal to the case A values of Table 8, of changing P_C only, and of changing V_{ref} only, respectively. The second and third figures show that V_{ref} is the more effective control as predicted by the larger sensitivities in Table 8.)

Eigenvalues λ	Eigenvalue Sensitivities with respect to P_C	
	$\frac{\partial \lambda}{\partial P_C}$ (rectangular)	(polar)
-49.5006	-0.0160	
0.0000±4.4518i	13.0447∓12.5675i	18.1137∠∓0.7668
-1.3875±4.0715i	-13.0611±8.5572i	15.6147∠±2.5616
-5.1825	-0.1308	
-4.2404	-0.2863	
-1.9772	-0.0171	
-0.0997	0.0000	
-0.8775	0.0770	

Table 4: Eigenvalues and sensitivities with respect to P_C at Hopf bifurcation
($P_C=1.1497$ p.u., $V_{ref}=0.9547$ p.u.)

Predicted eigenvalue	Actual eigenvalue	Error
-49.5005	-49.5005	0
-0.0842±4.5329i	-0.0823±4.5410i	-0.0019∓0.0081i
-1.3031±4.0162i	-1.3051±4.0079i	0.0020±0.0083i
-5.1816	-5.1816	0
-4.2385	-4.2385	0
-1.9772	-1.9772	0
-0.0997	-0.0997	0
-0.8780	-0.8780	0

Table 5: Eigenvalues when P_C is changed by -0.0065 predicted
using sensitivities from Table 4
($P_C=1.1432$ p.u., $V_{ref}=0.9547$ p.u.)

Eigenvalues λ	Eigenvalue Sensitivities with respect to V_{ref}	
	$\frac{\partial \lambda}{\partial V_{ref}}$ (rectangular)	(polar)
-49.5006	-0.1733	
0.0000±4.4518i	-29.8675±33.0416i	44.5400∠±2.3058
-1.3875±4.0715i	29.2586∓21.1092i	36.0786∠∓0.6250
-5.1825	0.3906	
-4.2404	1.2467	
-1.9772	0.1351	
-0.0997	0.0003	
-0.8775	-0.1590	

Table 6: Eigenvalues and sensitivities with respect to V_{ref} at Hopf bifurcation
($P_C=1.1497$ p.u., $V_{ref}=0.9547$ p.u.)

Predicted eigenvalue	Actual eigenvalue	Error
-49.5010	-49.5010	0
-0.0681±4.5271i	-0.0662±4.5326i	-0.0019∓0.0055
-1.3208±4.0234i	-1.3227±4.0177i	0.0019±0.0057
-5.1816	-5.1816	0
-4.2375	-4.2375	0
-1.9770	-1.9770	0
-0.0997	-0.0997	0
-0.8778	-0.8778	0

Table 7: Eigenvalues when V_{ref} is changed by 0.0023 predicted
using sensitivities from Table 6
($P_C=1.1497$ p.u., $V_{ref}=0.9570$ p.u.)

Equilibrium	P_C	V_{ref}	Critical Eigenvalues
A	1.14324	0.96043	$-0.2028 \pm j4.7868$
B	1.1497	0.9547	$0.0000 \pm j4.4518$
C	1.15338	0.95122	$0.1523 \pm j4.3125$

Equilibrium	Eigenvalue Sensitivities with respect to P_C	
	(rectangular)	(polar)
A	$6.6470 \mp j17.7442$	$18.9484 \angle \mp 1.2124$
B	$13.0447 \mp j12.5675$	$18.1137 \angle \mp 0.7668$
C	$12.5583 \mp j9.1529$	$15.5398 \angle \mp 0.6298$

Equilibrium	Eigenvalue Sensitivities with respect to V_{ref}	
	(rectangular)	(polar)
A	$-13.8344 \pm j44.4898$	$46.5912 \angle \pm 1.8723$
B	$-29.8675 \pm j33.0416$	$44.5400 \angle \pm 2.3058$
C	$-29.2235 \pm j24.7951$	$38.3251 \angle \pm 2.4380$

Table 8: Critical eigenvalues and their sensitivities equilibria A,B,C

6 37 Bus Equivalent Results

This section presents results for a 37 bus equivalent system. The results do not show feasibility of the proposed approach.

6.1 37 bus equivalent test case system and data

The test case system used for the remaining tasks is a 37 bus equivalent furnished by the New York Power Pool. The furnished data is given in Appendix A. The data was modified to fit the general model of Section 2. The modified data is given in Appendix B. The modifications were made to utilize the software developed to compute the system multi-machine eigenvalues. For purposes of evaluating robustness, this modified model represents the “inaccurately modeled” system as proposed in Task 4. The modifications included changes in all exciter and automatic voltage regulator models to match the IEEE Type I given in Section 2 and the addition of turbine/governor dynamics as shown in Section 2. Static VAR compensators and power system stabilizers were not modeled.

6.2 Eigenvalue analysis for load increase

The following results were obtained using the data of Appendix B with the model of Section 2. The following models were used for system loads:

$$P_{Li} = P_{LOi} V_i^{n_p} \quad (68)$$

$$Q_{Li} = Q_{LOi} V_i^{n_q} \quad (69)$$

For constant power loads ($n_p = 0, n_q = 0$), the system was unstable with the following modes in the right-half plane:

$$\begin{aligned} &+1.92 \pm j3.01 \\ &+0.13 \pm j3.69 \end{aligned}$$

For constant current loads ($n_p = 1, n_q = 1$), the system was stable (all eigenvalues in the left-half plane). The two modes of interest from above were,

$$\begin{aligned} &-.0029 \pm j5.03 \\ &-.0009 \pm j2.531 \end{aligned}$$

To examine the impact of increasing load, the load data of Appendix B was considered 100%. The real power output of each generator and the real and reactive powers of each load were increased by a factor to indicate load growth with corresponding generation increase. At a percent loading of 101% (with $n_p = n_q = 1$), the system became unstable with the following eigenvalues in the right-half plane:

$$\begin{aligned} &+.0248 \pm j4.99 \\ &+.0010 \pm j2.52 \end{aligned}$$

Attempts to stabilize the system using operator controls were only partially successful. The software for computing the eigenvalue sensitivities did not produce reliable results. Participation factors were used to guide the choice of possible effective controls. Increasing the output of generator 2 by 1% gave the following eigenvalues:

$$\begin{aligned} &+.0101 \pm j5.008 \\ &+.0088 \pm j2.52 \end{aligned}$$

This indicates that raising the output of generator 2 might stabilize one mode. Using this predicted sensitivity, a 3% increase in generator 2 output gave the following eigenvalues:

$$\begin{aligned} &-.022 \pm j5.04 \\ &+.024 \pm j2.51 \end{aligned}$$

The eigenvalues moved as predicted, stabilizing the first mode, but destabilizing the second. Lowering the output to 98% of its initial value gave the following eigenvalues:

$$\begin{aligned} &+.050 \pm j4.94 \\ &-.015 \pm j2.52 \end{aligned}$$

Again, the eigenvalues moved as predicted, stabilizing the second mode, but destabilizing the first.

6.3 Eigenvalue analysis - line outage

The following results were obtained using the data of Appendix B with the model of Section 2. Simulation of the system showed that load flow convergence was lost for a large number of line outages. Outage of line 15-19 did not cause load flow divergence and resulted in the following unstable modes (100% load, $n_p = n_q = 1$):

$$\begin{aligned} &+.0707 \pm j4.72 \\ &+.0036 \pm j2.53 \end{aligned}$$

Attempts to stabilize the system using operator controls were partially successful. Lowering the output of generator 2 to 98% resulted in the following eigenvalues:

$$\begin{aligned} &+.0656 \pm j4.65 \\ &-.0113 \pm j2.54 \end{aligned}$$

The first eigenvalue moved slightly to the left and the second was stabilized as in the last section. Lowering generator 2 further to 96% gave the following eigenvalues:

$$\begin{aligned} &+0.0545 \pm j4.56 \\ &-.0263 \pm j2.54 \end{aligned}$$

Lowering generator 2 further to 92% gave the following eigenvalues:

$$\begin{aligned} &+.0744 \pm j4.3 \\ &-.0534 \pm j2.54 \end{aligned}$$

The linear prediction in the movement of the first eigenvalue has failed. This 8% reduction caused the eigenvalue to reverse direction and become more unstable.

7 Computational Issues

Based on our experience with the 37 bus equivalent system, the computational requirements for computing eigenvalue sensitivities to operator control parameters will be very intense. The reason for this is primarily in the need to compute all of the Hessian matrices associated with the sensitivity of the operating point. This is equivalent to computing N load flow Jacobians for an N -bus system. While numerical sensitivities may be feasible using incremental parameter changes with corresponding incremental eigenvalue changes, this also has computational issues. Each incremental change would require the computation of the equilibrium point for fixed operator controls. This is not a standard load flow, and such software is not commercially available.

Timing runs on a Sun workstation indicate that it takes about 6 minutes to compute a subset of eigenvalues on a 4000 bus system. A numerical sensitivity would require at least two such solutions for each operator control. Assuming an operator has over 100 possible controls, this means the computation time on a Sun workstation would take $2 \times 6 \times 100 = 1,200$ minutes (20 hours). Even with advances in computing software and hardware, this does not appear feasible for the near future.

8 Conclusions

The concept of using eigenvalue sensitivities to predict proper operator controls was shown to be viable on a single machine/infinite bus test case. Every aspect of the analysis from analytical sensitivities through nonlinear simulation indicated that the basic approach to avoidance and elimination of sustained oscillations is feasible. In the 37 bus equivalent test case the results showed that there can be situations where the eigenvalue sensitivity information is unreliable. It is unreliable because the necessary controls predicted may be too large to be in the region where linear prediction is accurate. Furthermore, instabilities can occur

with multiple modes in the right-half plane and operator controls which stabilize one mode can destabilize another. This means that any ranking of controls must consider the impact of the control on all eigenvalues, not just the one or two that show an instability. Computational issues indicate that the time needed to compute all operator-control options will be very large. After this phase of the investigation, we cannot claim that the approach is feasible. We will continue our investigation into these issues without further funding requests. Should any reliable solutions to these problems emerge, we will provide the results to all interested persons in ESEERCO and NYSEG.

References

- [1] E.H. Abed, P.P. Varaiya, "Nonlinear oscillations in power systems," *International Journal of Electric Energy and Power Systems*, vol. 6, no. 1, Jan. 1984, pp. 37-43.
- [2] R. T. Byerly, R. J. Bennon and D. E. Sherman, "Eigenvalue analysis of synchronizing power flow oscillations in large electric power systems," *IEEE Transactions on Power Apparatus and Systems*, vol. PAS-101, January 1982, pp. 235-243.
- [3] R. C. Burchett and G. T. Heydt, "Probabilistic methods for power system dynamic stability studies," *IEEE Transactions on Power Apparatus and Systems*, vol. PAS-97, no. 3, May/June 1978, pp. 695-702.
- [4] J.H. Chow, A. Gebreselassie, Dynamic voltage stability of a single machine constant power load system, 29th IEEE CDC conference, Honolulu HI, Dec. 1990, pp. 3057-3062.
- [5] I. Dobson, L. Lu, Computing an optimum direction in control space to avoid saddle node bifurcation and voltage collapse in electric power systems, *IEEE Transactions on Automatic Control*, vol 37, no. 10, October 1992, pp. 1616-1620.
- [6] I. Dobson, Fernando Alvarado and C. L. DeMarco, "Sensitivity of Hopf bifurcations to power system parameters," Proceedings of the 31st Conference on Decision and Control, Tucson, Arizona, December 1992.
- [7] I. Dobson, Computing a closest bifurcation instability in multidimensional parameter space, *Journal of Nonlinear Science*, vol. 3, no. 3, 1993, pp. 307-327.
- [8] G. Golub, C. VanLoan, Matrix Computations, Johns Hopkins Universtiy Press, Baltimore, 1983.
- [9] G. Gross, C. F. Imparato and P. M. Look, "A tool for the comprehensive analysis of power system dynamic stability," *IEEE Transactions on Power Apparatus and Systems*, vol. PAS-101, no. 1, January 1982.
- [10] P. Kundur, G. J. Rogers, D. Y. Wong, L. Wang and M. G. Lauby, "A comprehensive computer program package for small signal stability analysis of power systems," *IEEE Transactions on Power Systems*, vol. PWRS-5, no. 4, November 1990, pp. 1076-1083.
- [11] D. M. Lam, H. Yee and B. Campbell, "An efficient improvement of the AESOPS algorithm for power system eigenvalue calculation," *IEEE Transactions on Power Systems*, vol. 9, no. 4, November 1994, pp. 1880-1885.

- [12] N. Martins, "Efficient eigenvalue and frequency response methods applied to power system small-signal stability studies," *IEEE Transactions on Power Systems*, vol. PWRS-1, no. 1, 1986, pp. 217-226.
- [13] J. E. Van Ness, J. M. Boyle and F. P. Imad, "Sensitivities of large multi-loop control systems," *IEEE Transactions on Automatic Control*, vol. AC-10, 1965, pp. 308-318.
- [14] P. Nolan, N. Sinha and R. Alden, "Eigenvalue sensitivities of power systems including network and shaft dynamics," *IEEE Transactions on Power Apparatus and Systems*, PAS-95, pp. 1318-1324, 1976.
- [15] F. L. Pagola, I. J. Perez-Arriaga and G. C. Verghese, "On sensitivities, residues and participants: Applications to oscillatory stability analysis and control," *IEEE Transactions on Power Systems*, vol. PWRS-4, no. 1, 1989, pp. 278-285.
- [16] M. A. Pai, K. R. Padiyar and P. S. Shetty, "Sensitivity based selection of control parameters for multi-machine power systems," Abstract in *IEEE Transactions on Power Apparatus and Systems*, PAS-99, 1980, p. 1320.
- [17] P. W. Sauer, C. Rajagopalan and M. A. Pai, "An explanation and generalization of the AESOPS and PEALS algorithms," *IEEE Transactions on Power Systems*, vol. 6, no. 1, February 1991, pp. 293-299.
- [18] R. Seydel, *From equilibrium to chaos: practical bifurcation and stability analysis*, Elsevier, New York OR the second edition Springer-Verlag, New York, 1994.
- [19] Thomas Smed, "Feasible eigenvalue sensitivity for large power systems," *IEEE Transactions on Power Systems*, vol. 8, no. 2, May 1993, pp. 555-563.
- [20] N. Uchida and T. Nagao, "A new eigen-analysis method of steady-state stability studies for large power systems: S matrix method," *IEEE Transactions on Power Systems*, PWRS-3, no. 2, May 1988, pp. 706-714.
- [21] L. Wang and A. Semlyen, "Application of sparse eigenvalue techniques to the small signal stability analysis of large power systems," *IEEE Transactions on Power Systems*, vol. PWRS-5, pp. 635-642, May 1990.
- [22] D. Y. Wong, G. J. Rogers, B. Poretta and P. Kundur, "Eigenvalue analysis of very large power systems," *IEEE Transactions on Power Systems*, PWRS-3, no. 2, pp. 472-480, May 1988.
- [23] L. Xu and S. Ahmed-Zaid, "Tuning of power system controllers using symbolic eigensensitivity analysis and linear programming," *IEEE Transactions on Power Systems*, vol. 10, no. 1, Feb. 1995, pp. 314-321.
- [24] EPRI Final Report, "Application of taxonomy theory," Part I: Research Project 3573-10, April 1995, prepared by Washington University in St. Louis, System Science and Mathematics, St. Louis, Missouri.
- [25] E. Zhou, S. Chen, Y. Ni and B. Zhang, "Modified selective analysis method and its application in the analysis of power system dynamics," *IEEE Transactions on Power Systems*, vol. 6, no. 3, August 1991, pp. 1189-1195.

A Appendix A

The attached pages list the 37 bus equivalent data in PTI raw format.

THE FOLLOWING PAGES MAY BE OBTAINED FROM THE AUTHORS

B Appendix B

The attached pages list the modified 37 bus equivalent data in format for the University of Illinois simulation.

In order to run this model with the software being used at the University of Illinois it was necessary to renumber the system buses as shown below:

<u>UI#</u>	<u>NYPP#</u>
1	4305
2	1
3	51
4	136
5	1459
6	2458
7	2812
8	2833
9	2834
10	2855
11	2864
12	3517
13	3520
14	3523
15	3645
16	3814
17	4611
18	4656
19	4895
20	5525
21	5890
22	5902
23	5903
24	6321
25	6597
26	6632
27	6659
28	6660
29	9484
30	1377
31	3864
32	4383
33	4387
34	5506
35	5685
36	5686
37	6188

THE FOLLOWING PAGES MAY BE OBTAINED FROM THE AUTHORS